FULL PAPER

Dalton
www.rsc.org/dalton

Chiral hexarhodium carbonyl clusters containing heterobidentate phosphine ligands; a structural and reactivity study

Sergey P. Tunik,*[a] Igor O. Koshevoy,[a] Anthony J. Poë,*[b] David H. Farrar,[b] Ebbe Nordlander,*[c] Matti Haukka[d] and Tapani A. Pakkanen

[a] *Department of Chemistry, St. Petersburg University, Universitetskii pr., 2, St. Petersburg, 198904, Russian Federation. E-mail: stunik@st1323.spb.edu*

[b] *Lash Miller Chemical Laboratories, University of Toronto, 80 St. George Street, Toronto, Ontario, Canada M5S 3H6. E-mail: apoe@ chem.utoronto.ca*

[c] *Inorganic Chemistry, Centre for Chemistry and Chemical Engineering, Lund University, Box 124, SE-221 00 Lund, Sweden. E-mail: Ebbe.Nordlander@inorg.lu.se*

[d] *Department of Chemistry, University of Joensuu, P.O. Box 111, FIN-80101 Joensuu, Finland*

Received 23rd January 2003, Accepted 23rd April 2003
First published as an Advance Article on the web 13th May 2003

Some intrinsically chiral $[Rh_6(CO)_{14}(\mu,\kappa^2\text{-PX})]$ clusters have been synthesized, beginning with reactions of $[Rh_6(CO)_{16-x}(NCMe)_x]$ (x = 1, 2) with PX, where PX represents the bidentate bridging ligands diphenyl(benzothienyl)phosphine (**1**), diphenyl(2-thienyl)phosphine (**2**), di(2-thienyl)phenylphosphine (**3**), tris(2-thienyl)phosphine (**4**), diphenyl(2-pyridyl)phosphine (**5**) and diphenylvinylphosphine (**6**). The ligand tris(2-furyl)phosphine (**7**) shows no bridging capability. When x = 1 the initial products are the clusters $[Rh_6(CO)_{15}(\kappa^1\text{-PX})]$ which undergo spontaneous CO loss to form $[Rh_6(CO)_{14}(\mu,\kappa^2\text{-PX})]$. The structures of the $[Rh_6(CO)_{15}(\kappa^1\text{-PX})]$ clusters have been elucidated by IR, NMR spectroscopy and FAB-MS spectrometry, and have been found to involve phosphorus atom coordination to a rhodium atom. In addition, the solid state structures of the $[Rh_6(CO)_{14}(\mu,\kappa^2\text{-}Ph_2P(2\text{-benzothienyl}))]$ (**8**), $[Rh_6(CO)_{14}(\mu,\kappa^2\text{-}Ph_2P(2\text{-thienyl}))]$ (**9**), $[Rh_6(CO)_{14}(\mu,\kappa^2\text{-PhP(2-thienyl)}_2)]$ (**10**) and $[Rh_6(CO)_{14}(\mu,\kappa^2\text{-}Ph_2P(\text{pyridyl}))]$ (**12**) clusters have been determined by X-ray crystallography. The various types of chirality exhibited by these clusters are discussed. A simple model is proposed to account for the ratios of stereochemical isomers found in the $Rh_6(CO)_{14}(\mu,\kappa^2\text{-PhP(2-thienyl)}_2$ cluster. The kinetics of formation of the bridged clusters from the monosubstituted $[Rh_6(CO)_{15}(\kappa^1\text{-PX})]$ clusters have been studied.

Introduction

Organometallic compounds containing functionalised phosphines are important for several reasons. The presence of a second coordinating atom or group provides a diversity of coordination modes that can lead to stereochemical differences in the final products of their reactions. Differences in dynamic behaviour that are attributable to the relative weakness of binding of the second coordinating atom or group to the metal are also important in leading to "hemilability"[1] and all these differences are of special interest when the ligands are bound to metal cluster frameworks. They open the way to targeted structural modification of complexes and to controlled reactivity that is especially important in catalytic applications. The chemistry of transition metal complexes containing X-functionalised P-donor ligands (PX), where X is a two electron donor containing sulfur, nitrogen or oxygen atoms, or a C=C double bond, has been investigated quite intensively for both mononuclear,[2–6] and cluster compounds.[7–24] From the viewpoint of structural chemistry, coordination of these potentially heterobidentate ligands to a cluster core can occur in various ways: chelating, bridging or in a simple κ^1 mode, usually through the phosphorus atom. Each of these is governed by particular properties of the ligand and metal centre or centres, as well as by particular mechanistic features of the ligand coordination process. Asymmetry of the various components can give rise to formation of isomeric product complexes and stereoisomers can, in principle, be formed, especially with bridging ligands. For example, bridging heterobidentate (X–Y) ligands positioned out of a metal triangular face form a chiral structural pattern, which has been successfully resolved for orthometallated pyridine derivatives.[25a] The diastereomers of Os_3 clusters containing orthometallated (*S*)-nicotine and (*R*)-1-(4-pyridyl)ethanol ligands displayed clear photophysical evidence of the chirality of the Os_3(X–Y) fragments in their CD spectra.[25a] The possible presence of several chiral centres in cluster molecules of this sort makes them particularly interesting from the viewpoint of catalytic applications provided that they are stereochemically rigid and maintain the asymmetry under the conditions of a catalytic experiment. A combination of all the features mentioned above makes these studies especially challenging for getting better insight into this field of cluster chemistry. In the present paper we report the reactions of the labile $[Rh_6(CO)_{16-x}(NCMe)_x]$ clusters (x = 1, 2) with Ph_2P(2-thienyl), $PhP(2\text{-thienyl})_2$, $P(2\text{-thienyl})_3$, Ph_2P(2-benzothienyl), Ph_2P-(2-pyridyl), Ph_2P(vinyl) and $P(2\text{-furyl})_3$ ligands. Structural characterization, by X-ray crystallography and NMR spectroscopy, of the generally bridged products, together with the kinetics of the PX bridge closure from initially formed $[Rh_6(CO)_{15}(\kappa^1\text{-PX})]$ clusters, are also described.

Experimental

General comments

The acetonitrile substituted clusters $[Rh_6(CO)_{16-x}(NCMe)_x]$ (x = 1, 2) were synthesized as described earlier.[26] Diphenyl(benzothienyl)phosphine (**1**) was synthesised by the reaction of the lithium salt of benzothiophene with PPh_2Cl.[27] The PX ligands diphenyl(2-thienyl)phosphine (**2**),[28] and di(2-thienyl)-phenylphosphine (**3**),[29] were prepared according to published procedures. Tris(2-thienyl)phosphine (**4**) (Lancaster), diphenyl-(2-pyridyl)phosphine (**5**) (Aldrich), diphenylvinylphosphine (**6**) (Aldrich) and tris(2-furyl)phosphine (**7**) (Lancaster) were used as received. All solvents (dichloromethane, chloroform, acetonitrile, hexane and diethyl ether (KEBO)) were distilled over appropriate drying agents under an atmosphere of nitrogen before use. Infrared spectra were recorded using a Nicolet Avatar 360 FTIR spectrometer. Fast atom bombardment (FAB+) mass spectra were obtained with a JEOL SX-102

DOI: 10.1039/b300951c

instrument; 3-nitrobenzyl alcohol was used as a matrix and CsI as the calibrant. The isotopic distribution patterns observed in the mass spectra fit completely to the calculated patterns. ^{1}H and ^{31}P NMR spectra were recorded on a Varian Unity 300 MHz spectrometer, and 2D ^{1}H–^{1}H COSY and HSQC spectra on a Bruker DRX 500C spectrometer. The chemical shifts were referenced to residual solvent resonances or external 85% H_3PO_4 in ^{1}H, ^{13}C and ^{31}P spectra, as appropriate. Thin layer chromatography was performed on commercial plates pre-coated with Merck Kieselgel, 60 to 0.5 mm thickness.

A general procedure for the synthesis and chromatographic purification of the mono-substituted $[Rh_6(CO)_{15}(\kappa^1\text{-PX})]$ and di-substituted $[Rh_6(CO)_{14}(\mu,\kappa^2\text{-PX})]$ clusters is exemplified below by the reactions of $[Rh_6(CO)_{16-x}(NCMe)_x]$ ($x = 1, 2$) with diphenyl(2-thienyl)phosphine (**2**). The yields of the new compounds, together with analytical and spectroscopic data, are given in Table 1.

Reaction of $[Rh_6(CO)_{15}(NCMe)]$ with (2). $[Rh_6(CO)_{15}(NCMe)]$ (40 mg, 0.037 mmol) was dissolved in dichloromethane (5 cm^3) and a slight excess (12 mg, 0.045 mmol) of **2** in dichloromethane (2 cm^3) was added to the cluster solution. Formation of the primary monosubstituted derivative, $[Rh_6(CO)_{15}(\kappa^1\text{-Ph}_2\text{P(2-thienyl)})]$ (**9′**), occurred almost immediately as verified by comparison of its IR and ^{31}P NMR spectra to those of known $[Rh_6(CO)_{15}(\kappa^1\text{-phosphine})]$ clusters.[24,30,31] The reaction mixture was left under nitrogen at room temperature for 10 h and both spectroscopic techniques showed complete conversion of **9′** into the final reaction product $[Rh_6(CO)_{14}(\mu,\kappa^2\text{-Ph}_2\text{P(2-thienyl)})]$ (**9**). (Here and elsewhere we choose to distinguish the monosubstituted clusters by primed numbers, while the bridged version is referred to by the same, unprimed, number. The relationship between the ligand numbering and the cluster numbering is that the cluster with the ligand number x is given the cluster number $7 + x$, since there are seven ligands. Thus clusters **9′** and **9** contain ligand **2**.)

TLC separation using a hexane–chloroform (2 : 1 v/v) eluent gave one main brown band containing **9**. After separation of the brown material from the plate and removal of the solvent a brown crystalline powder of **9** was obtained (45 mg, 95%).

Reaction of $[Rh_6(CO)_{14}(NCMe)_2]$ with (2). $[Rh_6(CO)_{14}(NCMe)_2]$ (45 mg, 0.042 mmol) was dissolved in dichloromethane (10 cm^3). A slight excess of **2** (14 mg, 0.052 mmol) in dichloromethane (2 cm^3) was added to the cluster solution. Formation of **9** occurred almost immediately. Chromatographic separation of the reaction mixture was performed as described above to give one main band containing cluster **9** (48 mg, 91%).

Kinetics of the transformation of $[Rh_6(CO)_{15}(\kappa^1\text{-PX})]$ into $[Rh_6(CO)_{14}(\mu,\kappa^2\text{-PX})]$. Monodentate $[Rh_6(CO)_{15}(\kappa^1\text{-PX})]$ clusters were prepared *in situ* by reaction of a slight excess of a phosphine ligand with $[Rh_6(CO)_{15}(NCMe)]$. Typically, a weighed amount of the starting cluster and phosphine were separately dissolved in toluene. The solutions were left for *ca.* 10–15 min at room temperature to allow complete dissolution of $[Rh_6(CO)_{15}(NCMe)]$. The ligand and cluster solutions were then mixed and immediately transferred into a pre-thermostated IR cell or, in the case of UV-Vis monitoring, small aliquots of the starting solutions were transferred into a pre-thermostated UV-Vis cell containing pure solvent. Time-dependent IR spectra were recorded on a Nicolet 550 Magna FTIR spectrophotometer in absorbance mode in the temperature-controlled infrared cell (Wilmad Glass, 2 mm pathlength) equipped with NaCl windows. Rate constants were obtained by monitoring the decrease in absorbances of the well separated IR bands at *ca.* 2100 cm^{-1} corresponding to $[Rh_6(CO)_{15}(\kappa^1\text{-PX})]$. Alternatively, and more generally, UV-Vis monitoring was carried out using Hewlett Packard 8452A diode array and Cary 300 Bio spectrophotometers. UV-Vis cells were thermostated using a Lauda RCS-6 thermostat bath. Absorbance changes were monitored at at least three wavelengths in the range 400–460 nm. Rate constants were obtained by single exponential analysis of the absorbance changes at each wavelength and averaged to give values of k_{obs}.

Good agreement was obtained between rate constants obtained from the different methods of monitoring. Convenient temperature ranges were selected for each cluster and at least five runs were carried out over a 25 °C temperature range. Activation parameters were obtained by unweighted linear least-square analysis of the dependence of $\ln(k_{obs}/T)$ on $1/T$, and estimates of the standard errors in k_{obs} ($\sigma(k_{obs})$ (%)) were determined from the scatter of the values of $\ln(k_{obs}/T)$ around the linear Eyring plot.

Isolation of crystals, X-ray data collection, and structure solution. Single crystals of **8**, **9**, **10**, **12** and **14** suitable for an X-ray study were grown by slow diffusion of heptane into chloroform solutions at 5 °C. The X-ray diffraction data were collected with a Nonius Kappa CCD diffractometer using Mo-Kα radiation ($\lambda = 0.71073$ Å) and the Collect data collection program.[32] The Denzo-Scalepack[33] program package was used for cell refinements and data reduction. All structures were solved by direct methods using the SHELXS97 program.[34] Structural refinements were carried out with the SHELXL97 program.[34] An empirical absorption correction based on equivalent reflections was applied to structure **9** (T_{min}/T_{max}: 0.25713/0.28486). The hydrogens in **8**, **10**, **12** and **14** were placed in idealised positions and constrained to ride on their parent atom. All hydrogens in **9** were located from the difference Fourier map and refined isotropically. Structures of **9** and **10** were refined as racemic twins with absolute structure parameter 0.30(2) and 0.18(2), respectively. In the structure **10** the thermal parameters indicated that S(2) and C(122) are possibly disordered over two sites in one of the S-containing rings. However, modelling of the disorder did not improve the result and therefore it was not applied for the structure solution. The crystallographic data are summarised in Table 2 and selected bond lengths and angles are shown in Table 3. The solid state structure of **13** has been recently obtained and will be published elsewhere.

CCDC reference numbers 202051–202055.

See http://www.rsc.org/suppdata/dt/b3/b300951c/ for crystallographic data in CIF or other electronic format.

Results and discussion

Synthesis and characterization of the $[Rh_6(CO)_{15}(\kappa^1\text{-PX})]$ clusters and the kinetics of their reactions to form the $[Rh_6(CO)_{14}(\mu,\kappa^2\text{-PX})]$ clusters

The reaction of $[Rh_6(CO)_{15}(NCMe)]$ has previously been used for the synthesis of various monosubstituted $[Rh_6(CO)_{15}L]$ derivatives,[24,30,31] which were completely characterized by various spectroscopic methods and X-ray crystallography. Thus, the same reaction with any one of the phosphines **1**–**7** affords, in the first stage, a monodentate phosphine substituted product $[Rh_6(CO)_{15}(\kappa^1\text{-PX})]$ in nearly quantitative yield, as verified by IR and ^{31}P spectroscopy. In the case of ligands **1**–**6**, the resultant monosubstituted Rh_6 clusters are unstable with respect to PX bridge closure and that prevents their complete characterization by separation and crystallography. Chromatographic isolation of the initial products **8′** and **9′** was initially quite clean but, on elution and isolation of the solid clusters, some bridge closure (<~10%) had occurred as evidenced by the ^{31}P NMR spectra. Nevertheless, the FAB mass spectra of these mixtures gave strong parent molecular ion peaks corresponding to $[Rh_6(CO)_{15}(PX)]$. Further, in **14′**, the P,O ligand **7** proved unable to undergo P,O bridge closure and this allowed X-ray structural characterization of the $[Rh_6(CO)_{15}(P(2\text{-furyl})_3)]$

Table 1 Spectroscopic data for the clusters **8′**–**14′** and **8**–**13**

Compound	IR (CH_2Cl_2) ν(CO)/cm^{-1}	Yield (%)	*m*/*z* (FAB)[a]	$\delta(^{31}P)$/ppm (*J*/Hz) ($CDCl_3$)	$\delta(^{1}H)$/ppm (*J*/Hz) ($CDCl_3$)
$[Rh_6(CO)_{15}(\kappa^1\text{-}Ph_2P(SC_8H_5)]$ (**8′**)	2100w, 2065s, 2036w, 2010vw, 1789m, br		1356 (1356), loss of 15 CO	18.2, dm, ^1J(Rh–P) 136.7	
$[Rh_6(CO)_{14}(\mu,\kappa^2\text{-}Ph_2P(SC_8H_5)]$ (**8**)	2092m, 2061s, 2031m, 2011w, 1775m, br	96.0	1328 (1328), loss of 14 CO	14.4, dm, ^1J(Rh–P) 140.6, ^2J(Rh–P) 4.0 and 1.7	7.98 (m, 1H), 7.77 (m, 1H), 7.66 (m, 1H), 7.60 (m, 1H), 7.58–7.48 (m, 10H, Ph), 6.74 (d, ^1J(P–H) 6, 1H)
$[Rh_6(CO)_{15}(\kappa^1\text{-}Ph_2P(SC_4H_3)]$ (**9′**)	2099w, 2065s, 2034w, 2008vw, 1789m, br		1306 (1306), loss of 15 CO	16.8, dm, ^1J(Rh–P) 139.2	
$[Rh_6(CO)_{14}(\mu,\kappa^2\text{-}Ph_2P(SC_4H_3)]$ (**9**)	2092m, 2062s, 2033m, 2011w, 1778m, br	95.0	1278 (1278), loss of 14 CO	12.5, dm, ^1J(Rh–P) 139.6, ^2J(Rh–P) *ca*. 4.0	7.94 (t, *J* 4.4, 1H), 7.68–7.40 (m, 10H, Ph), 7.32 (dd, *J* 5.5, 3.3, 1H), 6.49 (dd, *J* 6.6, 3.3, 1H)
$[Rh_6(CO)_{15}(\kappa^1\text{-}PhP(SC_4H_3)_2)]$ (**10′**)	2100w, 2064s, 2035w, 2008vw, 1795m, br			6.2, d ^1J(Rh–P) 141.9	
$[Rh_6(CO)_{14}(\mu,\kappa^2\text{-}PhP(SC_4H_3)_2)]$ (**10a**)[b]	2092m, 2060s, 2030m, 2008w, 1784m, br	92.0 (**a** + **b**)	1284 (1284), loss of 14 CO	3.88, d ^1J(Rh–P) 144.0	7.96 (t, *J* 4.9, 1H, c), 7.69 (dd, *J* 4.9, 2.9, 1H, nc),[c] 7.67–7.45 (m, Ph), 7.62 (dm, *J* 6.8, 1H, nc), 7.36 (m, 1H, c), 7.25 (m, 1H, nc), 6.64 (dd, *J* 6.8, 3.4, 1H, c)
$[Rh_6(CO)_{14}(\mu,\kappa^2\text{-}PhP(SC_4H_3)_2)]$ (**10b**)[b]				−2.85, d ^1J(Rh–P) 142.8	8.12 (dd, *J* 7.8, 3.5, 1H, nc), 7.91 (t, *J* 4.7, 1H 134, c), 7.73 (dm, *J* 5.9, 1H, c),[b] 7.67–7.45 (m, Ph), 7.38 (m, 1H, nc), 7.31 (dd, *J* 4.6, 3.4, 1H 133, c), 6.67 (dd, *J* 5.9, 3.4, 1H 132, c)
$[Rh_6(CO)_{15}(\kappa^1\text{-}P(SC_4H_3)_3)]$ (**11′**)	2099w, 2064s, 2035w, 2009vw, 1796m, br			−1.3, dm, ^1J(Rh–P) 146.5	
$[Rh_6(CO)_{14}(\mu,\kappa^2\text{-}P(SC_4H_3)_3)]$ (**11**)	2092m, 2060s, 2030m, 2009w, 1782m, br	92.0	1290 (1290), loss of 14 CO	−10.4, dm, ^1J(Rh–P) 147.4	6.76 (dd, *J* 6.3, 3.4, 1H), 7.23 (m, 1H), 7.34 (m, 2H), 7.62 (dd, *J* 7.32, 3.4, 1H), 7.71 (m, 2H), 7.92 (t, *J* 4.4, 1H), 8.07 (dd, *J* 8.3, 3.4)
$[Rh_6(CO)_{15}(\kappa^1\text{-}Ph_2P(C_5H_4N))]$ (**12′**)	2099w, 2064s, 2035w, 2005vw, 1792m, br			20.1, d ^1J(Rh–P) 135.5	
$[Rh_6(CO)_{14}(\mu,\kappa^2\text{-}Ph_2P(C_5H_4N))]$ (**12**)	2089m, 2057s, 2026m, 2003w, 1778m, br	91.0	1245(1273), loss of 13 CO	24.6, d ^1J(Rh–P) 144.7	9.22 (d, *J* 5.37, 1H), 7.75 (tm, *J* 7.81), 7.61–7.36 (m, 11H), 7.28 (dm, *J* 8.19, 1H)
$[Rh_6(CO)_{15}(\kappa^1\text{-}Ph_2P(C_2H_3))]$ (**13′**)	2099w, 2065s, 2034w, 2009vw, 1795m, br			20.0, dm ^1J(Rh–P) 131.9	
$[Rh_6(CO)_{14}(\mu,\kappa^3\text{-}Ph_2P(C_2H_3))]$ (**13**)	2094m, 2063s, 2032m, 2009w, 1789m, br	91.4	1222 (1222), loss of 14 CO	16.9, d ^1J(Rh–P) 125.5	7.83 (m, 2H (Ph)), 7.73 (m, 2H (Ph)), 7.45 (m, 6H (Ph)), 5.00 (dd, *J*(P–H) 26.9 and *J*(H–H) 9.6, 1H), 4.54 (dt, *J*(H–H) 9.6 and 13.7, 1H), 3.54 (t, *J*(H–H) 13.7, 1H)
$[Rh_6(CO)_{15}(\kappa^1\text{-}P(2\text{-}OC_4H_3))]$ (**14**)	2100w, 2065s, 2036w, 1796m, br	89.0	1270 (1270), loss of 15 CO	−19.2, dt, ^1J(Rh–P) 147.4, ^2J(Rh–P) 4.6	7.65 (m, 3H), 6.77 (m, 3H), 6.45 (m, 3H)[d]

[a] Molecular ion in parentheses. [b] All the spectra for these compounds were run using the mixture of isomers. In the ^{31}P NMR spectra two doublets of relative intensity 1 : 1.9 were observed and this ratio was used to assign clearly separated low field and high field signals in the ^1H NMR spectrum. [c] This multiplet contains the signals of both **a** and **b** isomers. [d] In CD_2Cl_2.

Table 2 Crystallographic data for compounds **8**, **9**, **10**, **12** and **14**

	8	**9**	**10**	**12**	**14**
Empirical formula	$C_{34}H_{15}O_{14}PRh_6S$	$C_{30}H_{13}O_{14}PRh_6S$	$C_{28}H_{11}O_{14}PRh_6S_2$	$C_{31}H_{14}NO_{14}PRh_6$	$C_{27}H_9O_{18}PRh_6$
M_w	1327.95	1277.89	1283.92	1272.86	1269.77
Crystal system	Monoclinic	Monoclinic	Monoclinic	Triclinic	Monoclinic
Space group	$P2_1/c$	$P2_1$	$P2_1$	$P\bar{1}$	$P2_1/n$
a/Å	11.7069(3)	9.62700(10)	9.4304(19)	9.906(2)	9.8477(4)
b/Å	19.2614(8)	17.1463(3)	16.894(3)	11.924(2)	34.1917(13)
c/Å	17.2961(7)	11.3747(2)	11.371(2)	15.821(3)	10.2373(4)
α/°	90	90	90	91.53(3)	90
β/°	97.240(2)	106.3520(10)	105.34(3)	94.34(3)	103.297(2)
γ/°	90	90	90	105.66(3)	90
V/Å^3	3869.0(2)	1801.64(5)	1747.1(6)	1792.2(6)	3354.6(2)
T/K	150(2)	293(2)	150(2)	100(1)	100(1)
Z	4	2	2	2	4
D_c/g cm^{-3}	2.280	2.356	2.441	2.359	2.514
μ/mm^{-1}	2.661	2.852	2.999	2.811	3.011
No. refl. collected	13363	29500	20812	27652	17296
No. unique refl.	6795	7904	6109	8196	5899
R_{int}	0.0483	0.0300	0.0266	0.1310	0.0690
$R1$ [a]	0.0404	0.0210	0.0225	0.0503	0.0493
$wR2$ [a]	0.0663	0.0497	0.0568	0.0876	0.0874

[a] $I > 2\sigma$.

cluster. Even reaction of one equivalent of **7** with $[Rh_6(CO)_{14}(NCMe)_2]$ does not afford the bridging species. Instead, **14′** and the disubstituted $[Rh_6(CO)_{14}(\kappa^1\text{-}P(2\text{-furyl})_3)_2]$ cluster, characterized spectroscopically, are formed. The evidence is therefore incontrovertible that, in all cases, the initial products of the reactions are the simple monosubstituted carbonyl clusters with P-donor PX ligands.

The initial coordination of the functionalised phosphine *via* the phosphorus atom occurs rapidly as expected from the lability of the acetonitrile complex and the greater donicity of the phosphorus atom as compared with the hetero atoms or group. This is followed by coordination of the S, N or double bond functions to a rhodium atom next to the one coordinated by the phosphorus so that the product is formed in the μ,κ^2-bonding mode. The latter reaction is very smooth as evidenced by the good isosbestic points shown by the IR traces in Fig. 1. This indication of the cleanness of the reactions allows us to be sure that UV-Vis monitoring will also give reliable rate constants. The absorbance changes in the 420–460 nm range of the UV-Vis spectra fit very well to single exponential analyses and the averaged rate constants are given in Table 4. These are independent of the concentration of any free phosphine ligand, showing that the reactions clearly involve an intramolecular displacement of a CO ligand. The activation parameters, also shown in Table 4, were derived from the rate constant changes over substantial temperature ranges. The precision of the activation parameters is excellent and the fit to the Eyring analysis shows that the precision of the individual rate constants is very good.

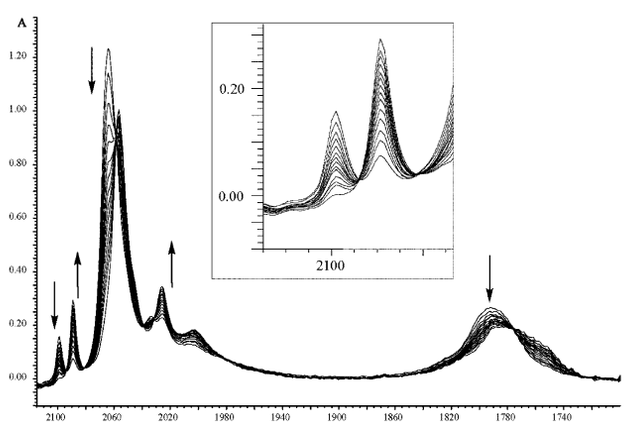

Fig. 1 Changes in the IR spectra during bridge closure reaction in $Rh_6(CO)_{15}(\kappa^1\text{-}Ph_2P$ (2-pyridyl) in CH_2Cl_2 at 32.8 °C.

The highest value of $\Delta S^{\ddagger}$ (*ca.* +22 cal K^{-1} mol^{-1}) is quite compatible with a simple CO dissociative rate-determining step.[35] This suggests that the incipient $[Rh_6(CO)_{14}(\mu\text{-}Ph_2P(vinyl))]$ that is formed as the CO dissociates does not undergo the sort of "cluster tightening" that is often postulated to cause less positive values of $\Delta S^{\ddagger}$ in reactions of smaller metal carbonyl clusters.[36–38] Since the absence of this phenomenon seems unlikely to be dependent on the detailed nature of the ligand, we can ascribe the less positive value $\Delta S^{\ddagger}$ for $[Rh_6(CO)_{15}(Ph_2P(pyridyl))]$ to a genuine contribution from bond-making in the transition state.[39] The essentially pure dissociative mechanism for $[Rh_6(CO)_{15}(Ph_2P(vinyl))]$ would be in accord with the low nucleophilicity expected for the vinyl group in the ligand. On the other hand, the suggestion of some associative character for the reaction of $[Rh_6(CO)_{15}(Ph_2P(pyridyl))]$ is compatible with nucleophilic attack at the C atom of a nearby CO, hard nucleophiles being well known to react in this way.[35] The associative contribution is not particularly large by comparison with the bridge-closing reaction of $[Os_3(CO)_{11}(\kappa^1\text{-dppm})]$,[41] for which $\Delta S^{\ddagger} = -10$ cal K^{-1} mol^{-1}, but it does appear to be finite. Associative contributions to the reactions of the clusters with thienyl-containing phosphine ligands appear to be very small.

Synthesis and structural characterization of the $[Rh_6(CO)_{14}(\mu,\kappa^2\text{-PX})]$ clusters

The instability towards CO loss, in solution, of the monosubstituted clusters **8′**–**13′** allows facile formation of the corresponding stable $[Rh_6(CO)_{14}(\mu,\kappa^2\text{-PX})]$ clusters containing a five-membered Rh–P–C–X–Rh ring (X = S, **8**–**11**; N, **12**; or a C=C group, **13**). The same products can be obtained by reaction of the corresponding phosphine with $[Rh_6(CO)_{14}(NCMe)_2]$ which can provide an easily generated second coordination vacancy for coordination of the X-atom or group. This reaction affords the bridged clusters immediately in nearly quantitative yield. All these simple bridged complexes contrast with the more complex products, involving oxidative addition *etc.*, found in studies of related but smaller clusters.[10,11,19–23]

In contrast to $[Rh_6(CO)_{14}(\mu,\kappa^2\text{-P(pyrrolyl)}_3)]$,[40] none of the clusters **8**–**12** reacts with CO (25 °C, 1 atm of CO) to restore the initial κ^1 coordination of the phosphine, and this suggests substantially more effective X-group bonding to the Rh_6 skeleton as compared with the P(pyrrolyl)$_3$ ligand. It turns out, however, that the relative lability of $[Rh_6(CO)_{14}(\mu,\kappa^2\text{-P(pyrrolyl)}_3)]$ is due

Table 3 Selected bond lengths (Å) and angles (°) in $[Rh_6(CO)_{14}((\mu,\kappa^2\text{-PX})]$ clusters (PX = $Ph_2P(C_8H_5S)$ **8**, $Ph_2P(C_4H_3S)$ **9**, $PhP(C_4H_3S)_2$ **10**, $Ph_2P(C_5H_4N)$ **12**). For numbering scheme, see Fig. 1

	8	**9**	**10**	**12**	**14**	
Rh–Rh						
Rh(10)–Rh(20)	2.7815(8)	2.7762(3)	2.7648(8)	2.7763(14)	2.8132(9)	
Rh(10)–Rh(21)	2.7667(8)	2.7538(3)	2.7525(7)	2.7615(15)	2.7852(9)	
Rh(10)–Rh(30)	2.7554(8)	2.7784(4)	2.7709(7)	2.7688(13)	2.7894(9)	
Rh(10)–Rh(31)	2.7558(8)	2.7433(4)	2.7377(11)	2.7608(13)	2.7622(9)	
Rh(20)–Rh(21)	2.7434(8)	2.7492(3)	2.7496(7)	2.7036(10)	2.7715(9)	
Rh(30)–Rh(31)	2.7726(8)	2.7830(4)	2.7881(8)	2.7843(11)	2.7561(9)	
Rh(20)–Rh(30)	2.7800(7)	2.7708(4)	2.7636(8)	2.7949(12)	2.7439(10)	
Rh(21)–Rh(31)	2.7130(7)	2.7264(4)	2.7275(8)	2.7130(13)	2.7361(10)	
Rh(40)–Rh(30)	2.7315(8)	2.7402(4)	2.7451(7)	2.7390(15)	2.7582(9)	
Rh(40)–Rh(31)	2.7855(8)	2.7954(4)	2.7956(8)	2.7989(14)	2.7591(10)	
Rh(40)–Rh(20)	2.7901(8)	2.7994(3)	2.7867(11)	2.7825(13)	2.7483(10)	
Rh(40)–Rh(21)	2.7322(8)	2.7229(3)	2.7152(7)	2.7312(13)	2.7665(10)	
Average [a]	**2.7590(248)**	**2.7616(259)**	**2.7581(250)**	**2.7596(313)**	**2.7658(215)**	
Rh–μ_3-CO						
Rh(40)–C(10)O	2.208(7)	2.234(3)	2.237(5)	2.185(9)	Rh(10)–C(10)O	2.162(9)
Rh(20)–C(10)O	2.205(8)	2.186(3)	2.183(6)	2.183(9)	Rh(20)–C(10)O	2.204(9)
Rh(21)–C(10)O	2.160(7)	2.168(3)	2.183(5)	2.128(9)	Rh(21)–C(10)O	2.243(9)
Rh(10)–C(20)O	2.199(8)	2.183(4)	2.180(5)	2.202(8)	Rh(20)–C(20)O	2.180(9)
Rh(20)–C(20)O	2.144(8)	2.136(3)	2.128(6)	2.128(9)	Rh(30)–C(20)O	2.222(9)
Rh(30)–C(20)O	2.284(8)	2.288(4)	2.280(6)	2.259(10)	Rh(40)–C(20)O	2.182(9)
Rh(10)–C(21)O	2.202(8)	2.248(4)	2.249(5)	2.209(8)	Rh(10)–C(11)O	2.109(9)
Rh(21)–C(21)O	2.131(8)	2.090(3)	2.086(5)	2.084(8)	Rh(30)–C(11)O	2.196(9)
Rh(31)–C(21)O	2.303(8)	2.264(4)	2.240(5)	2.273(10)	Rh(31)–C(11)O	2.247(9)
Rh(40)–C(30)O	2.199(7)	2.204(4)	2.203(7)	2.185(10)	Rh(40)–C(30)O	2.239(10)
Rh(30)–C(30)O	2.186(8)	2.169(4)	2.173(6)	2.176(10)	Rh(21)–C(30)O	2.189(10)
Rh(31)–C(30)O	2.189(8)	2.185(4)	2.208(6)	2.166(10)	Rh(31)–C(30)O	2.191(9)
Average [a]	**2.201(50)**	**2.196(56)**	**2.196(53)**	**2.182(53)**		**2.197(39)**
Rh–CO_t						
Average [a]	**1.903(13)**	**1.895(10)**	**1.900(15)**	**1.889(15)**	**1.900(10)**	
Rh–P						
Rh(20)–P(1)	2.3142(18)	2.3216(8)	2.3098(15)	2.308(3)	Rh(10)–P(1)	2.311(2)
Rh(21)–X [b]	2.3747(18)	2.3907(9)	2.3928(15)	2.162(7)		
P–Rh–Rh						
P(1)–Rh(20)–Rh(21)	93.70(5)	93.81(2)	93.57(4)	88.72(6)		
X–Rh(21)–Rh(20)	92.57(5)	93.24(2)	93.79(4)	92.63(16)		
P(1)–Rh(20)–Rh(10)	102.13(5)	100.39(2)	99.66(4)	97.01(7)		
X–Rh(21)–Rh(10)	92.60(5)	93.79(2)	93.78(4)	100.38(18)		
P(1)–Rh(20)–Rh(40)	140.03(5)	141.01(2)	141.25(4)	138.55(7)		
X–Rh(21)–Rh(40)	147.17(5)	147.11(2)	147.56(4)	141.66(17)		
P(1)–Rh(20)–Rh(30)	157.03(5)	155.47(2)	154.62(4)	153.99(7)		
X–Rh(21)–Rh(31)	144.99(5)	145.74(2)	145.24(4)	153.58(18)		
Bond lengths in dimetallocycle						
P(1)–C(131)	1.790(7)	1.808(3)	1.810(5)	1.845(8)		
X–C(131)	1.775(7)	1.736(4)	1.752(5)	1.367(10)		
Angles in dimetallocycle						
Rh(20)–P(1)–C(131)	108.0(2)	107.51(11)	108.23(17)	111.5(3)		
Rh(21)–X–C(131)	103.0(2)	103.83(11)	103.44(17)	123.1(5)		
P(1)–C(131)–X	116.4(4)	118.99(19)	118.8(3)	117.4(6)		

[a] Values of variance $S = [(x_i - \bar{x})^2/(n-1)]^{1/2}$ for the averages are given in parentheses. [b] (X = S for **8**, **9**, **10**; N for **12**).

to an exceptionally unfavourable intrinsic entropy of this cluster, compared with the nonbridged $[Rh_6(CO)_{15}(\kappa^1\text{-P-(pyrrolyl)}_3)]$, which overcomes the contribution of entropy loss due to transformation of a free CO ligand into a bound one. The Rh–C bond in $[Rh_6(CO)_{14}(\mu,\kappa^2\text{-P(pyrrolyl)}_3)]$ is at least as strong, enthalpically, as the Rh–CO bond it replaces.[40] A small amount of **13** is transformed into **13′** under CO but this reaction, and those of some other disubstituted Rh_6 clusters, will be described in detail elsewhere.

The thienylphosphine clusters. In previous studies of ruthenium, osmium and cobalt clusters, analogues of ligands

Table 4 Rate constants and activation parameters ($\Delta H^{\ddagger}$/kcal mol^{-1}, $\Delta S^{\ddagger}$/cal K^{-1} mol^{-1}) for the ring closure reactions in the clusters $Rh_6(CO)_{15}L$

Ph_2P(Pyridyl)		Ph_2P(Vinyl)		Ph_2P(Thienyl)		$PhP(Thienyl)_2$		$P(Thienyl)_3$	
T/°C	10^3k_{obs}/s^{-1}	T/°C	10^3k_{obs}/s^{-1}	T/°C	10^3k_{obs}/s^{-1}	T/°C	10^3k_{obs}/s^{-1}	T/°C	10^3k_{obs}/s^{-1}
25.9	0.067	25.3	0.026	25.0	0.071	29.5	0.131	28.0	0.091
31.3	0.131	30.8	0.075	29.5	0.154	39.5	0.61	39.4	0.52
31.6	0.142	35.2	0.144	39.5	0.72	44.0	1.25	45.4	1.29
35.7	0.22	41.6	0.380	49.0	3.04	49.0	2.53	51.5	2.95
39.8	0.39	46.0	0.85	54.0	5.34	54.0	4.37	56.6	6.07
46.4	1.07	48.5	1.14						
53.0	2.58								
$\Delta H^{\ddagger} = 26.2 \pm 0.6$		$\Delta H^{\ddagger} = 30.4 \pm 0.6$		$\Delta H^{\ddagger} = 28.5 \pm 0.5$		$\Delta H^{\ddagger} = 27.9 \pm 0.7$		$\Delta H^{\ddagger} = 28.3 \pm 0.2$	
$\Delta S^{\ddagger} = 9.8 \pm 2.0$		$\Delta S^{\ddagger} = 22.3 \pm 1.9$		$\Delta S^{\ddagger} = 18.1 \pm 1.5$		$\Delta S^{\ddagger} = 15.9 \pm 2.2$		$\Delta S^{\ddagger} = 16.8 \pm 0.6$	
$\sigma(k_{obs}) = 9.9\%$		$\sigma(k_{obs}) = 6.4\%$		$\sigma(k_{obs}) = 5.2\%$		$\sigma(k_{obs}) = 6.7\%$		$\sigma(k_{obs}) = 2.1\%$	

1–**4** were usually found to give either κ^1 coordination through phosphorus,[7–9,42] or, in the case of $[M_3(CO)_{12}]$ derivatives, coordination to all three metals of the triangular cluster through the phosphorus and a metallated thienyl ring in σ–π vinyl coordination mode.[10] In contrast, clusters **8′**–**11′**, containing the κ^1-coordinated thienyl-substituted phosphines **1**–**4** undergo facile bridge closure *via* coordination of the sulfur atoms to yield clusters **8**–**11**.

The molecular structures of **8** and **9** are shown in Fig. 2, that of **10** in Fig. 3, and selected bond distances and bond angles are

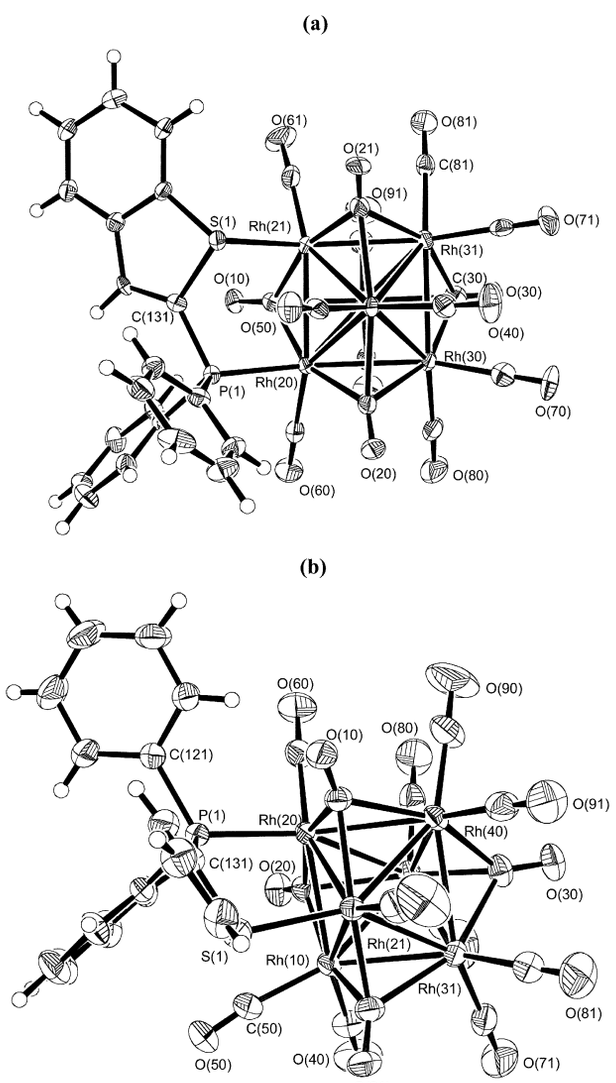

Fig. 2 ORTEP plots of the molecular structures of (a) $[Rh_6(CO)_{14}(\mu,\kappa^2\text{-}Ph_2P(2\text{-benzothienyl}))]$ (**8**) and (b) $[Rh_6(CO)_{14}(\mu,\kappa^2\text{-}Ph_2P(2\text{-thienyl}))]$ (**9**) showing the atom labelling scheme. Thermal ellipsoids are drawn at the 50% level.

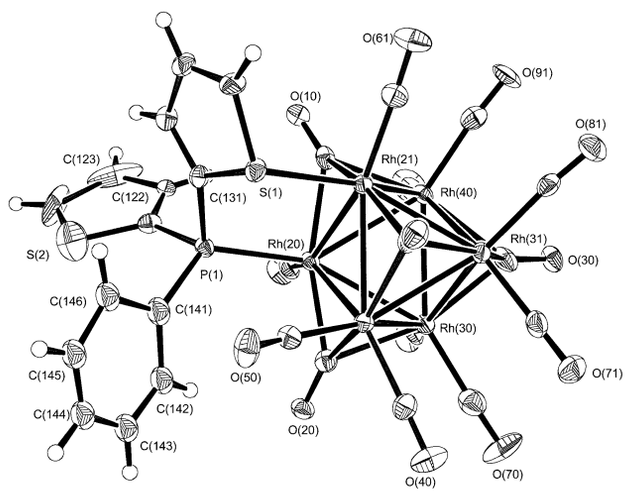

Fig. 3 ORTEP plots of the molecular structures of $[Rh_6(CO)_{14}(\mu,\kappa^2\text{-}PhP(2\text{-thienyl})_2)]$ (**10**). Thermal ellipsoids are drawn at the 50% level.

listed in Table 3. The clusters $[Rh_6(CO)_{14}(\mu,\kappa^2\text{-}Ph_2P(2\text{-benzothienyl}))]$ (**8**) and $[Rh_6(CO)_{14}(\mu,\kappa^2\text{-}Ph_2P(2\text{-thienyl}))]$ (**9**) are virtually isostructural with respect to the phosphorus-thienyl moieties and the $\{Rh_6(CO)_{14}\}$ fragments. In **8**, the average Rh–Rh distance is 2.759 Å, while in **9** it is 2.762 Å (*cf.* $[Rh_6(CO)_{16}]$, $Rh–Rh_{av}$ = 2.75(1) Å[31]). It has been noted that in $[Rh_6(CO)_{15}(L)]$ clusters (L = phosphine, phosphite, cyclooctene), the distortions of the idealized T_d symmetry of the $[Rh_6(CO)_{16}]$ cluster are fairly localized.[31] Thus, the two bonds between the substituted metal and the two Rh atoms that are *cis* to the ligand show a pronounced lengthening and the two Rh–Rh bonds that are in relative *trans* position to the ligand are the second longest.[31] Quite different local effects of the coordinated phosphorus and sulfur atoms are observed in **8** and **9**. In both **8** and **9**, the two metal–metal vectors *trans* to the phosphine are elongated [**8**: Rh(20)–Rh(30) 2.7800(7) Å, Rh(20)–Rh(40) 2.7901(8) Å; **9**: Rh(20)–Rh(30) 2.7708(4) Å, Rh(20)–Rh(40) 2.7994(3) Å], whereas the "*cis*-effect" is much less pronounced as compared with the monosubstituted $[Rh_6(CO)_{16}]$ derivatives.[31] In contrast, the two bonds in relative *trans* position to the thienyl sulfur are shortened. In **8**, they are 2.7130(7) Å [Rh(21–Rh(31)] and 2.7322(8) Å [Rh(21)–Rh(40)] and similar distances are observed for **9**. The rhodium–phosphorus distances (Table 3) are similar to those observed for monosubstituted phosphine derivatives of $[Rh_6(CO)_{16}]$[31,43]

Comparison of the various bond angles with those in $[Rh_6(CO)_{16}]$[31] indicate almost unstrained conformation of the five-membered "dimetallacycles" that are formed *via* the didentate coordination of the thienyl phosphine ligands, and the metal–metal bonds that are bridged by the ligands are only slightly shorter than the average Rh–Rh distance for each cluster. The Rh(21)–S(1) bonds are *ca.* 110° out of the thienyl ring plane, suggesting lone pair donation from nearly sp^3 hybridized sulfur atoms [*cf.* Figs. 2 and 3]. This geometry has also been

found in $[Re_2(CO)_8((\mu\text{-}P,S\text{-}Ph_2PC_4H_3S)]$,[11] $[Os_3(\mu\text{-}H)(CO)_7\{\mu_3\text{-}Ph_2P(C_8H_4S)\}\{\mu_2\text{-}Ph_2P(C_8H_5S)\}]$,[44] as well as in other complexes containing coordinated thiophene.[11,45,46] The μ,κ^2-(P,S) coordination mode is rare for thienyl-substituted phosphines; to our knowledge, the only other known examples of such coordination in metal carbonyl clusters are the above-mentioned dincuclear rhenium complex and triosmium cluster. The precise stereoelectronic effects of the bite angle of the thienyl-phosphorus system, and the donor ability of the thienyl sulfur atom, both play a decisive role in the ability of these PX ligands to bridge two adjacent rhodium atoms in the Rh_6 clusters. For example, the reaction of the labile $[Rh(cyclooctadiene)_2]^+$ complex with **2**[47] results in substitution of one cyclooctadiene ligand to give $[Rh(cyclooctadiene)(Ph_2P(2\text{-thienyl}))_2]^+$ with κ^1 coordinated phosphines, whereas the reaction of the same starting complex with $Ph_2P(CH_2CH_2SCH_3)$ affords a compound in which the phosphine is chelated to the rhodium centre through the phosphorus and sulfur atoms. The facile formation of the P,S(thienyl) bridges in **8**–**11** and the stability of these clusters, originate most probably from the closely matched geometry of the P and S lone pairs in **1**–**4** with the terminal vacancies of adjacent rhodium atoms in the Rh_6 skeleton.

Spectroscopic data obtained for clusters **8** and **9** (*cf.* Table 1) show that the structure found in the solid state remains unchanged in solution. The ^{31}P spectra of both compounds display expected multiplets due to Rh–P coupling. In the ^1H NMR spectra the protons of the coordinated benzylthienyl and thienyl substituents appear as well separated and appropriate multiplets. For both compounds the structure of the phenyl multiplets indicates an inequivalence of two phenyl rings in accordance with the solid state structure. The absence of changes in the ^1H NMR spectrum of **9** upon heating to 55 °C also testifies to the rigidity of the coordination of the P,S fragment, which positions the two phenyl rings in clearly different stereochemical environments.

Reaction of $[Rh_6(CO)_{15}(NCMe)]$ with $PhP(2\text{-thienyl})_2$ afforded the $[Rh_6(CO)_{14}(\mu,\kappa^2\text{-}PhP(2\text{-thienyl})_2]$ cluster which crystallizes as a racemic twin mixture, and the ratio of enantiomers in the solid state has been estimated to be *ca*. 4 : 1. Like the analogous P,S phosphines in **8** and **9**, the ligand **3** in cluster **10** is coordinated in a bridging manner through the phosphorus and sulfur atom of a thienyl ring (Fig. 3). The main structural parameters of this molecule in the solid state closely resemble those found for **8** and **9** (see Table 3) and fall in the range typical for other substituted $Rh_6(CO)_{16}$ derivatives. It is worth noting that in **10** the elongation of the metal–metal vectors *trans* to the phosphorus atom is less pronounced than in **8** and **9** [Rh(20)–Rh(30) 2.7636(8) Å, Rh(20)–Rh(40) 2.7867(11) Å, $Rh–Rh_{av} \approx$ 2.76 Å], while shortening of the metal–metal bonds *trans* to the coordinated thienyl sulfur is quite significant [Rh(21)–Rh(31) 2.7275(8) Å, Rh(21)–Rh(40) 2.7152(7) Å].

In contrast to its analogues, the ^{31}P and ^1H NMR spectroscopic data of **10** showed that the cluster exists in solution as a mixture of what was found to be two regioisomers (*vide infra*). These are present in a 2 : 1 ratio, irrespective of the reaction conditions (25 and 50 °C) or the methods of attempted chromatographic separation, which included careful segmentation of the corresponding band. A detailed spectroscopic investigation of the isomeric mixture was undertaken to assign the structures of the isomers in solution. The 1D projection of the ^1H NMR spectrum of the mixture given in Fig. 4 allows assignment of a few well resolved low and high field signals to **10a** (major isomer) and **10b** (minor isomer) on the basis of their relative intensities. However, a complete assignment, which distinguishes the signals of coordinated thienyl rings from the noncoordinated thienyl and phenyl rings for each isomer, has been accomplished by 2D ^1H–^1H COSY and ^1H–^{13}C HSQC spectroscopy (Figs. 4 and 5). In accordance with the solid state structure shown in Fig. 3, the connectivities observed in the ^1H–^1H COSY spectrum in Fig. 4 make it possible to divide the signals of each

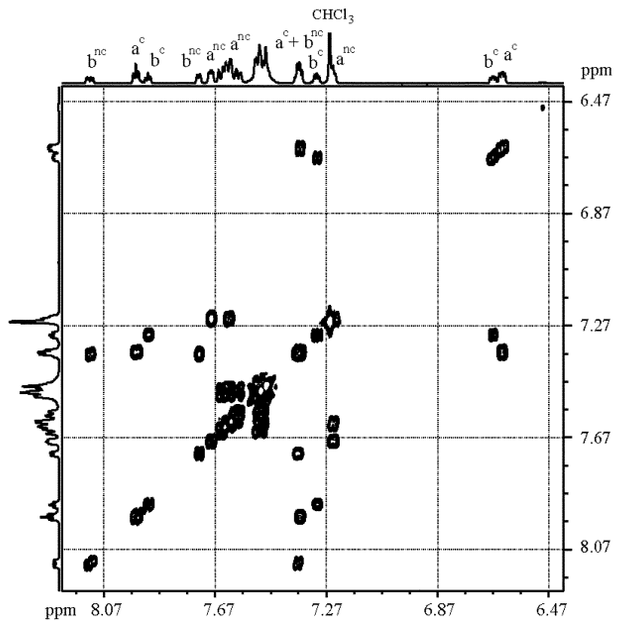

Fig. 4 ^1H COSY spectrum of the **10a** and **10b** mixture; superscripts ^{c} and ^{nc} in the numbering of signals refer to coordinated and noncoordinated thienyl rings.

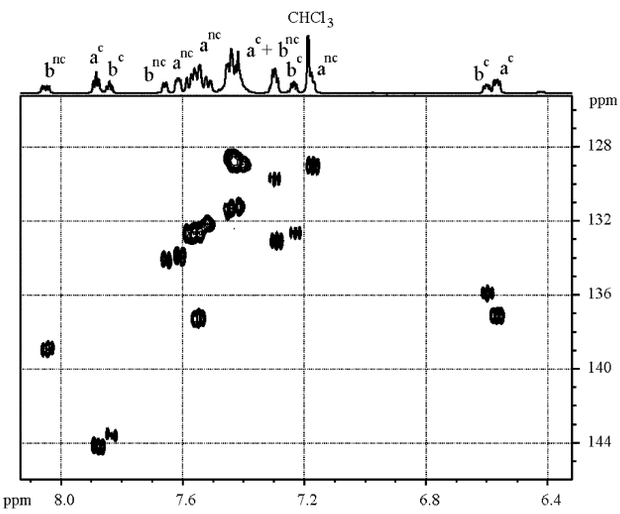

Fig. 5 ^1H-{^{13}C} HSQC spectrum of the **10a** and **10b** mixture, superscripts ^{c} and ^{nc} in numbering of signals refer to coordinated and noncoordinated thienyl rings.

isomer into three groups: those for two thienyl rings (three protons each) and another group of five signals belonging to a phenyl ring. The signals of the thienyl rings at 7.96 (t) and 6.64 (dd) ppm for **10a**, and at 7.91 (t) and 6.67 (dd) ppm for **10b**, look very similar in location and multiplicity to the spectroscopic pattern observed for the coordinated thienyl ring in **9** (7.94 (t) and 6.49 (dd) ppm). The similarity suggests assignment of the former resonances, as well as related signals found at 7.36 and 7.31 ppm, to coordinated thienyl moieties in **10a** and **10b**, respectively. In the case of the major isomer, **10a**, the resonances of the noncoordinated thienyl group at 7.69, 7.62, 7.25 ppm appear in the region that fits well to the thienyl signals of the free ligand. The minor isomer displays two analogous resonances at 7.73 and 7.38 ppm, but one low field shifted signal at 8.12 ppm, which lies outside the typical region for free thienyl ring protons. The corresponding ^{13}C resonance (139 ppm) is also shifted towards low field as compared with two other C(H) resonances of the same fragment (134 and 129 ppm as shown in Fig. 5). These data make it possible to assign the resonances of the major isomer to the structure found in the solid state where the noncoordinated thienyl ring is pointed

away from the cluster metal triangle to which the ligand is bound. The minor isomer should bear the bridging phosphine ligand with a slightly different stereochemistry. The most reasonable coordination geometry of the minor isomer, which fits the bridging ligand coordination and the spectroscopic data obtained, can be generated by exchange of noncoordinated phenyl and thienyl rings in the structure shown in Fig. 3. This operation brings the "free" thienyl ring into the position over the metal triangle and closer to adjacent carbonyl ligands. We believe that an explanation for the low field shifts of some signals in the ^{1}H and ^{13}C NMR spectra of the minor isomer might be the existence of hydrogen bonding between the α thienyl proton and the oxygen atom of the adjacent carbonyl ligand [C(20)O(20)]. In fact, the α proton (H(142)) of the phenyl ring in the major isomer has an extremely short nonbonding contact with O(20), 2.398 Å. It looks very probable that the α thienyl proton in the minor isomer has a similar nonbonding interaction with the bridging carbonyl that results in "hydrogen bonding" between two ligands and the observed low field shifts of the H(142) and C(142) signals in the NMR spectra.

The structure of the cluster $[Rh_6(CO)_{14}(\mu,\kappa^2\text{-}P(2\text{-thienyl})_3)]$, **11** has not been obtained crystallographically but it has been characterized by use of FAB MS, IR and various NMR spectroscopic methods. The data obtained (Table 1) clearly indicate the similarity of its structure to those found for the mono- and bis-(2-thienyl)phosphine derivatives, **9** and **10**. This similarity also confirms ligand coordination through the sulfur atom of a thienyl ring and the presence of the free, as well as the coordinated, thienyl rings.

The cluster $[Rh_6(CO)_{14}\{\mu,\kappa^2\text{-}Ph_2P(pyridyl)\}]$ (12). The solid state structure of the diphenylpyridylphosphine derivative **12** (Fig. 6), is closely analogous to those of the thienyl containing clusters **8**–**10**, and selected structural parameters of **12** are included in Table 2. The trend in Rh–Rh distances that is observed for the thienyl phosphine-subsituted clusters **8** and **9** is also observed for **12**. Thus, the two Rh–Rh bonds "*trans*" to the phosphorus [Rh(20)–Rh(40) and Rh(20)–Rh(30), *cf.* Table 3] are long while those "*trans*" to the nitrogen [Rh(21)–Rh(31) and Rh(21)–Rh(40)] are short. In contrast to **8** and **9**, the P,N-bridged bond in **12** is significantly shorter [Rh(20)–Rh(21) 2.7036(10) Å] than the average Rh–Rh bond length (2.76 Å), presumably because of the shorter "bite" of the P,N-ligand as compared with the thienyl containing phosphines. The five–membered nitrogen-containing ring forms a nearly planar N(1)Rh(21)Rh(20)P(1) system, the corresponding torsion angle being very small. However, the orientation of the pyridyl ring with respect to the Rh(21)–N(1) bond differs essentially from the geometry observed in the thienyl phosphine derivatives

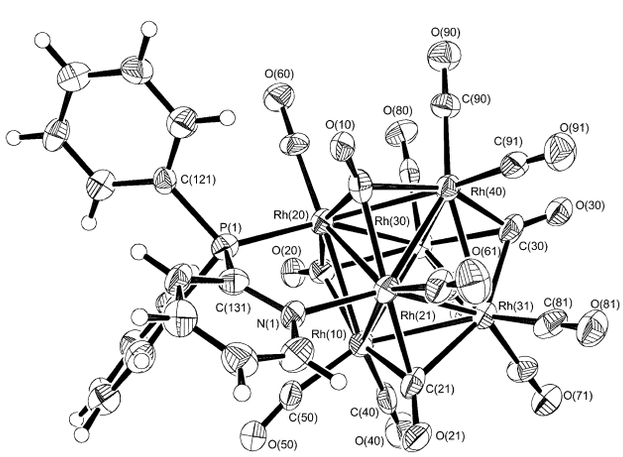

Fig. 6 ORTEP plot of the molecular structure of $[Rh_6(CO)_{14}\{\mu,\kappa^2\text{-}Ph_2P(pyridyl)\}]$ (**12**) showing the atom labelling scheme. Thermal ellipsoids are drawn at the 50% level.

8–**10**. The angle between the pyridyl ring plane and the Rh(21)–N(1) bond is much larger (*ca.* 160°) than the corresponding values in **8**–**10**. The difference in the orientation of the pyridyl and thienyl rings clearly demonstrates the difference in hybridization of the sulfur (sp^3) and nitrogen (sp^2) lone pairs involved in donation to the rhodium atoms, and thus the different degrees of aromaticity of the thienyl and pydridyl rings of the ligands. The Rh(20)–P(1) and Rh(21)–N(1) distances fall in the range usually observed for other P-donor substituted derivatives of $[Rh_6(CO)_{16}]$[31,43,48] and for other Rh–N bond lengths found in pyridylphosphine containing polynuclear rhodium complexes.[49–51] The spectroscopic data obtained for **12** (IR, ^{1}H, ^{31}P NMR, see Table 1) show that the structure found in the solid state remains unchanged in solution. The coordination mode of the bidentate ligand is also rigid on the NMR time scale because no changes in the proton NMR of the cluster were observed upon heating the cluster solution to 55 °C.

The cluster $[Rh_6(CO)_{14}(\mu,\kappa^2\text{-}Ph_2P(vinyl))]$ (13). Cluster **13** contains the diphenylvinylphosphine ligand **6**, where the vinyl double bond represents a potential second coordinating function. Reactions of **6** and analogous vinyl containing phosphines with trinuclear ruthenium and osmium clusters[22,23,52–54] initially afford κ^1(P)-coordinated ligands. In general, this type of coordination is rather stable for the trinuclear clusters and, in contrast to formation of **13**, removal of an additional CO requires thermolysis,[52,54] treatment with Me_3NO,[22] or activation by TLC plate material[23,53] or $[CpNi(CO)]_2$[23] before involvement of the vinyl moiety in bonding to the cluster core. One exception is $[Ru_3(CO)_{10}(Ph_2PCH{=}CH_2)_2]$ which is photosensitive and spontaneously forms $[Ru_3(\mu\text{-}H)(CO)_8(Ph_2PCH{=}CH_2)(\mu_2\text{-}Ph_2PCH{=}CH)]$ upon exposure to visible light at ambient temperature.[22] Two types of bridging structures have been observed in these cases. In one of them the vinyl fragment forms the bridge by coordination to an adjacent metal atom through the double bond which serves as a normal two-electron alkene donor.[23,52] The other bridging structure[22,23,53,54] results from oxidative addition of the vinyl moiety to give a hydride and a bridging $\{\mu,\kappa(P),\eta^2\text{-}P\text{–}CH\text{–}CH\}$ fragment. In the chemistry of $[Rh_6(CO)_{16}]$ derivatives, a close analogue of **13**, $[Rh_6(CO)_{14}(\mu\text{-}Ph_2P(allyl))]$, has been synthesized and structurally characterized.[24] In this allylphosphine cluster the double bond occupies a terminal position at an adjacent rhodium of the Rh_6 skeleton and forms a six-membered "dimetallacycle" without metallation of the organic moiety. The FAB mass spectrum of **13** displays the signal of the molecular ion, corresponding to the $[Rh_6(CO)_{14}\{Ph_2P(vinyl)\}]$ composition, and a fragmentation pattern corresponding to sequential loss of 14 CO ligands. The ^{31}P spectrum (Table 1) fits well to phosphorus coordination on the Rh_6 cluster core.[48,55] The IR spectroscopic pattern in the carbonyl region matches closely those found for other $[Rh_6(CO)_{14}(\mu,\kappa^2\text{-}PX)]$ clusters (Table 1), as well as that found for $[Rh_6(CO)_{14}\{Ph_2P(allyl)\}]$.[24] The ^{1}H spectrum of the vinyl moiety displays three typical multiplets of the vinyl protons and typical (^{1}H–^{1}H) and (^{31}P–^{1}H) couplings. A clear high field shift of the proton multiplets (as compared with the spectrum of the free ligand) points to vinyl coordination on the Rh centre. No signals have been found in the hydride region of the spectrum and this, in combination with the other spectroscopic data, testifies in favour of η^2 double bond coordination at an adjacent Rh atom without ligand metallation. The resolution of the proton multiplets in the range 7.9–7.4 ppm demonstrates the inequivalence of the two phenyl rings that is an evident result of their stereochemically different positions over the cluster skeleton.

The cluster $[Rh_6(CO)_{15}(\kappa^1\text{-}P(2\text{-furyl})_3)]$ (14′). As mentioned above, the tris(2-furyl)phosphine ligand, reacts with $[Rh_6(CO)_{15}(NCMe)]$ to give the monosubstituted $[Rh_6(CO)_{15}(\kappa^1\text{-}P(2\text{-furyl})_3)]$ cluster, **14′**. In contrast to all other $[Rh_6(CO)_{15}(\kappa^1\text{-}PX)]$

clusters described above, this compound is stable in solution with respect to bridge formation. The molecular structure of **14** is shown in Fig. 7 and selected structural data are given in Table 3. The structural parameters of this molecule (bond lengths, angles, distortions induced by insertion of the phosphine into the cluster coordination sphere) are in complete accordance with the regular structural features found earlier for other monosubstituted phosphine derivatives of $[Rh_6(CO)_{16}]$ (*vide supra*).[31] The spectroscopic data (Table 1) show that the structure found in the solid state remains unchanged in solution. The doublet of triplets observed in the ^{31}P NMR spectrum points to ligand coordination through phosphorus, whereas three typical 2-furyl multiplets in the proton NMR spectrum shows that three furyl rings are equivalent due to unhindered rotation of the phosphine about the Rh–P axis. Phosphine ligands containing 2-furyl substituents have not been widely used for synthesis of transition metal complexes. In three published structures, the oxygen of furyl substituents does not form either a chelate in mononuclear,[56,57] or a bridge in dinuclear,[58] complexes. These examples, along with the κ^1 coordination mode of **14′** found in the present study, provide clear evidence of the poor donor properties of the furyl oxygen with respect to low oxidation state metal centres as compared with the closely analogous sulfur atoms in thienyl rings.

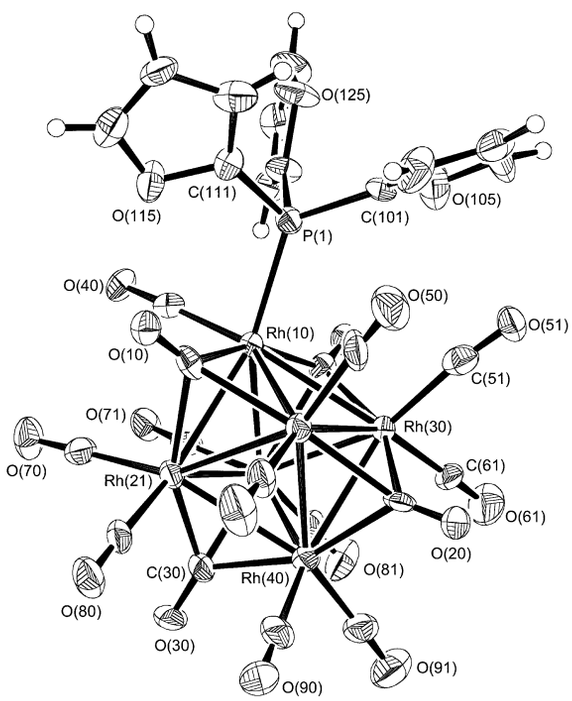

Fig. 7 ORTEP plot of the molecular structure of $[Rh_6(CO)_{15}(\kappa^2\text{-P-(2-furyl)}_3)]$ (**14′**) showing the atom labelling scheme. Thermal ellipsoids are drawn at the 50% level.

General stereochemical considerations

An important general feature of $[Rh_6(CO)_{14}(\mu,\kappa^2\text{-PX})]$ complexes and, indeed, of any cluster that contains a triangular group of metals with a bridging PX ligand occupying axial positions, is their intrinsic chirality which exists even in the absence of any chiral atomic centres. This type of asymmetry was first mentioned by Deeming *et al.*[25] with respect to trinuclear clusters containing bridging formamido, pyridine and pyrazine ligands. To relate this asymmetry to other chiral centres possibly presented in a cluster molecule, and to systematically assign its absolute configuration, it is necessary to use the Chan–Ingold–Prelog (CIP) rules.[59–61] These provide planar chirality nomenclature that is particularly convenient for making assignments in this particular case. Thus, in Fig. 8 the clusters **A** are enantiomeric because of the existence of the

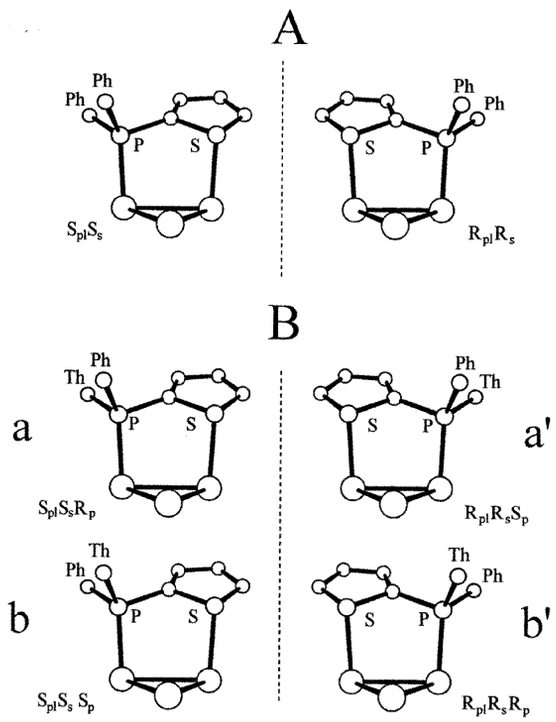

Fig. 8 Stereoisomers and chiral centers in the $\{Rh_3(\mu,\kappa^2\text{-PX})\}$ fragment. (A) (PX) = Ph_2P(2-Thienyl), (B) (PX) = $PhP(2\text{-Thienyl})_2$. Ph and Th refer to phenyl and 2-thienyl, respectively.

Rh–S–C–P–Rh connection and its position at approximately right angles to the Rh_3 plane. Choosing this plane as the basic reference for indexing clusters of this sort, the left hand enantiomer can be assigned as S_{pl} and the other as R_{pl} where the subscripts refer to the planar chirality of the fragments.

Choice of the highest molecular mass heteroatom in the PX ligand as the "out of plane" element is quite logical under the framework of the CIP system. The procedure for ranking the vertices in the pseudo-tetrahedral SRh_3 unit is then quite simple to give the $S_{pl}S_s$ and $R_{pl}R_s$ indexing for the two stereoisomers of the $[Rh_6(CO)_{14}(PS)]$ clusters shown in Fig. 8(A). These also possess another centre of asymmetry, *viz.* the S atom with three different bonds and one lone pair defining the classical tetrahedral asymmetry defined by R_s and S_s indexes. Because there are two chiral elements in the molecule there should, in principle, be four possible stereoisomers made up of two pairs of enantiomers connected to each other by a diastereomeric relationship. The pair not shown in Fig. 8(A) is the one where the carbon chain of the thienyl ring points towards the inner part of the Rh_3 triangle. This orientation is presumably sterically unfavourable because of substantial van der Waals interaction between the thienyl ring and the neighbouring C(50)O(50) ligand (see Fig. 3). For **8** and **9**, the NMR spectra indicated the existence of only one isomer (pair of enantiomers) and the crystal structures of the two clusters confirmed, in each case, the presence of the enantiomeric pair described above. It should be noted that the sp^2 hybridization of the nitrogen atom, verified by the nearly planar configuration of the coordinated pyridine ring and the Rh–N bond in **12**, results in the absence of any asymmetry at the nitrogen atom. In **13**, on the other hand, the α vinyl carbon is clearly chiral and makes the stereochemistry of this cluster similar to that of thienyl containing derivatives.

In the case of the phenyldithienylphosphine cluster **10**, there is a third chiral centre at the phosphorus atom where all four substituents are different (*cf.* Fig. 8(B)). A combination of three chiral centres in **10** should give rise to eight possible stereoisomers, four of which are shown in Fig. 8(B). The remaining four bear the unfavourable thienyl ring orientation described above, and may therefore be excluded from consideration. The

former allowed stereoisomers can be divided into two enantiomeric pairs ($R_{pl}R_sR_p$, $S_{pl}S_sS_p$ and $R_{pl}R_sS_p$, $S_{pl}S_sR_p$), each of which should display different spectroscopic properties. In fact, the mixture of stereoisomers obtained is indicated by the two sets of signals in the ^{1}H and ^{31}P NMR spectra, corresponding to **10a** and **10b** as discussed in detail above, and the X-ray analysis confirms the presence of the $R_{pl}R_sS_p$, $S_{pl}S_sR_p$ enantiopair in the solid state. This is in complete agreement with the existence of the two proposed diastereomeric forms for the cluster of this particular structure.

Another experimental observation relevant to the synthesis of the phenyldithienylphosphine derivatives also calls for rationalization. Determination of relative amounts of the **10a** and **10b** isomers by ^{1}H and ^{31}P NMR spectroscopy gave a 2 : 1 ratio irrespective of the methods of synthesis, the separation procedures applied or the reaction temperature. In particular, the VT ^{31}P spectra of the isomeric mixture showed that this ratio was retained in the temperature range (−10 to +50 °C) and we did not observe any line broadening of the phosphorus resonances corresponding to either of the isomers. This means that the isomeric forms of **10** are not in equilibrium with each other and that the ratio observed is related to the kinetics of their formation and to the particular structural features of the initial [$Rh_6(CO)_{15}(\kappa^1$-PPh_2(thienyl))] cluster. The following explanation can be suggested.

The four stereoisomers (**a**, **a′**, **b**, **b′**) of cluster **10** (Fig. 8(B)) are schematically shown in Fig. 9 in a Newman-type of projection from above the metal triangle, looking down the Rh–P bond. The κ^1 coordination of the phosphorus to a rhodium atom of the triangle gives rise to three possible orientations of the ligand with respect to the cluster skeleton. These modes are shown as **I**, **II** and **III**, which represent statistically averaged orientations of the phosphorus substituents inside three 120° sectors. Formation of each of the structures **I**, **II** and **III** is assumed to be equally probable. Provided that there are no hindrances for the phosphine rotation about the P–Rh(20) axis, when the vacancy for sulfur coordination is created on one of the two neighbouring Rh atoms, the least motions of the ligand for each of the A, B, C forms afford the corresponding stereoisomers in equal probability, as shown in Fig. 8. Thus movement of the bottom thienyl group to the left in **I** will give **a′** and movement to the right will give **b** and so on. This imaginary synthetic experiment, with purely geometrical constraints, gives rise to twice as many **a** or **a′** isomers as **b** or **b′** isomers. Thus, the 2 : 1 ratio of the racemic mixtures **a/a′** and **b/b′** isomers, as observed in the real experiments for the clusters **10a** and **10b**, can be rationalized in this very simple way. This approach provides additional arguments which support the structural assignments of the **10a** and **10b** isomers. However, as expected, this isomeric resolution is not accompanied by a chiral resolution.

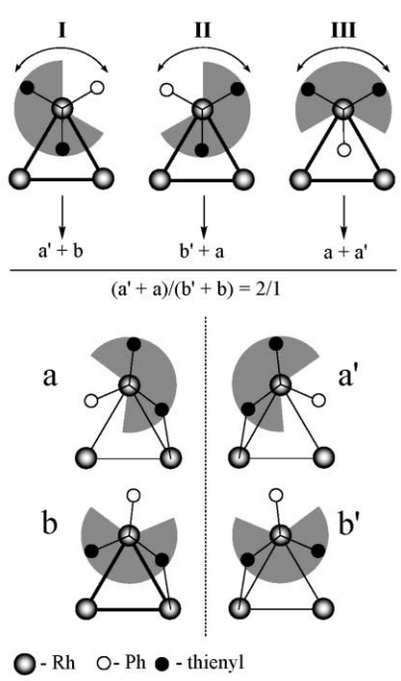

Fig. 9 Schematic presentation of the results of an imaginary synthetic experiment to generate the isomers of cluster **10**.

According to the proton NMR data, the compounds **8**–**12** are in fact stereochemically rigid in the temperature range 10–55 °C so that, in the light of the well known catalytic properties of the rhodium carbonyls in general, detailed investigation of their structure and reactivity would be especially attractive. Although all these clusters have been obtained in the form of racemic mixtures, exploitation of this type of cluster in chiral catalysis might be possible as shown, for example, by examples of asymmetric activation by racemic catalysts.[62–64] Moreover, a synthetic approach which consists of insertion of an additional molecule of an enantiomerically pure phosphorus donor into the coordination sphere of the cluster, or of modification of the PX ligand stereochemistry by replacing an achiral phosphorus substituent by one bearing a chiral centre, could also be used to attain a higher degree of stereoresolution in the final cluster complexes. A study of the corresponding chemistry is now in progress.

In conclusion, we have found that:

1. Interaction of labile [$Rh_6(CO)_{16-x}(NCMe)_x$] clusters ($x = 1$, 2) with some heterobidentate phosphine ligands results in PX bridge closure to give rise to [$Rh_6(CO)_{14}(\mu,\kappa^2$-PX)] clusters when X = S, N, or C=C. The initial step of κ^1 coordination of the ligand is followed by irreversible, or nearly irreversible, displacement of a CO (or, presumably, the second acetonitrile group) to form the final products. These reactions reveal a dramatic difference between donor properties of the thienyl and furyl groups towards metal atoms in a low oxidation state. The oxygen function of tris(2-furyl)phosphine does not afford the μ,κ^2 ligand bonding mode, locking the reaction at the end of the first stage.

2. The coordination of a functionalized phosphine in the bridging mode on the Rh_6 cluster core gives rise to a structural pattern containing centres of asymmetry, one of which is related to a planar chirality of the Rh_3 triangle bearing the PX ligand. In the case of the $PhP(2\text{-thienyl})_2$ ligand two (of the possible four) pairs of enantiomers have been formed in the ratio of 2 : 1. The stereoselection observed can be rationalized by taking into account simple geometrical constraints on the phosphorus ligand coordination and possible steric hindrances, which affect the coordinated thienyl ring orientation with respect to the cluster core.

3. The kinetics of bridge closure for the S, N and C=C containing ligands have been studied. The replacement of a CO ligand by the vinyl group in the κ^1-PPh_2(vinyl) complex is classically dissociative, as indicated by the substantially positive entropy of activation, with no need to invoke any entropic effects due to compensating tightening of the cluster bonding. By contrast, this suggests that there is a finite contribution of some sort of bond making in the case of the PPh_2(pyridyl) complex where the activation entropy is perceptibly less positive. The $PPh_n(thienyl)_{3-n}$ complexes are intermediate, and any associative character in their reactions seems to be minimal.

Acknowledgements

This research has been supported by grants from the Swedish Institute and Wenner-Gren Center Foundation (to S. P. T.), the Academy of Finland (to M. H. and T. A. P.), the Swedish Research Council (VR, to E. N.), the Natural Science and Engineering Research Council, Ottawa (to A. J. P and D. H. F), the Nordic Council of Ministers and the Royal Swedish Academy of Sciences.

References

1 P. Braunstein and F. Naud, *Angew. Chem., Int. Ed.*, 2001, **40**, 680.
2 J. R. Dilworth and N. Wheatley, *Coord. Chem. Rev.*, 2000, **199**, 89.
3 K. V. Katti, H. Gali, C. J. Smith and D. E. Berning, *Acc. Chem. Res.*, 1999, **32**, 9.
4 J. Bakos, B. Heil, L. Kollar and S. Toros, *Magy. Kem. Foly.*, 1994, **100**, 394.
5 O. A. Erastov and G. N. Nikonov, *Usp. Khim.*, 1984, **53**, 625.
6 T. B. Rauchfuss, *Homogeneous Catal. Met. Phosphine Complexes*, 1983, 239.
7 T. M. Rasanen, S. Jaaskelainen and T. A. Pakkanen, *J. Organomet. Chem.*, 1998, **553**, 453.
8 J. D. King, M. Monari and E. Nordlander, *J. Organomet. Chem.*, 1999, **573**, 272.
9 U. Bodensieck, H. Vahrenkamp, G. Rheinwald and H. Stoeckli-Evans, *J. Organomet. Chem.*, 1995, **488**, 85.
10 A. J. Deeming, S. N. Jayasuriya, A. J. Arce and Y. DeSanctis, *Organometallics*, 1996, **15**, 786.
11 A. J. Deeming, M. K. Shinhmar, A. J. Arce and Y. D. Sanctis, *J. Chem. Soc., Dalton Trans.*, 1999, 1153.
12 C. G. Arena, D. Drommi, F. Faraone, M. Lanfranchi, F. Nicolo and A. Tiripicchio, *Organometallics*, 1996, **15**, 3170.
13 M.-J. Don, K. Yang, S. G. Bott and M. G. Richmond, *J. Coord. Chem.*, 1996, **40**, 273.
14 F.-E. Hong, Y.-C. Chang, R.-E. Chang, C.-C. Lin, S.-L. Wang and F.-L. Liao, *J. Organomet. Chem.*, 1999, **588**, 160.
15 K. Wajda-Hermanowicz, F. Pruchnik and M. Zuber, *J. Organomet. Chem.*, 1996, **508**, 75.
16 K. Wajda-Hermanowicz, F. Pruchnik, M. Zuber, G. Rusek, E. Galdecka and Z. Galdecki, *Inorg. Chim. Acta*, 1995, **232**, 207.
17 K. Wajda-Hermanowicz, M. Koralewicz and F. P. Pruchnik, *Appl. Organomet. Chem.*, 1990, **4**, 173.
18 A. J. Deeming and M. B. Smith, *J. Chem. Soc., Chem. Commun.*, 1993, 844.
19 A. J. Deeming and M. B. Smith, *J. Chem. Soc., Dalton Trans.*, 1993, 2041.
20 A. J. Deeming and M. B. Smith, *J. Chem. Soc., Dalton Trans.*, 1993, 3383.
21 M. I. Bruce and M. L. Williams, *J. Organomet. Chem.*, 1986, **314**, 323.
22 B. F. G. Johnson, J. Lewis, E. Nordlander and P. R. Raithby, *J. Chem. Soc., Dalton Trans.*, 1996, 3825.
23 R. Giordano, E. Sappa, G. Predieri and A. Tiripicchio, *J. Organomet. Chem.*, 1997, **547**, 49.
24 S. I. Pomogailo, I. I. Chuev, G. I. Dzhardimalieva, A. V. Yarmolenko, V. D. Makhaev, S. M. Aldoshin and A. D. Pomogailo, *Russ. Chem. Bull.*, 1999, **48**, 1174.
25 (*a*) A. J. Deeming, M. J. Stchedroff, C. Whittaker, A. J. Arce, Y. De Sanctis and J. W. Steed, *J. Chem. Soc., Dalton Trans.*, 1999, 3289; (*b*) A. J. Arce and A. J. Deeming, *J. Chem. Soc., Chem. Commun.*, 1980, 1102.
26 S. P. Tunik, A. V. Vlasov and V. V. Krivykh, *Inorg. Synth.*, 1997, **31**, 239.
27 J. D. King, D. J. E., M. H. Johansson, B. F. G. Johnson, and E. Nordlander, unpublished resuls.
28 A. J. Arce, A. J. Deeming, Y. Desanctis, R. Machado, J. Manzur and C. Rivas, *J. Chem. Soc., Chem. Commun.*, 1990, 1568.
29 D. W. Allen and D. F. Ashford, *J. Inorg. Nucl. Chem.*, 1976, **38**, 1953.
30 A. J. Poë and S. P. Tunik, *Inorg. Chim. Acta*, 1998, **268**, 189.
31 D. H. Farrar, E. V. Grachova, A. Lough, C. Patirana, A. J. Poë and S. P. Tunik, *J. Chem. Soc., Dalton Trans.*, 2001, 2015.
32 Collect data collection software, B. V. Nonius, 1997–2000.
33 Z. Otwinowski and W. Minor, *Processing of X-ray Diffraction Data Collected in Oscillation Mode*, in *Methods in Enzymology, Volume 276, Macromolecular Crystallography, Part A*, ed. C. W. Carter, Jr. and R. M. Sweet, Academic Press, New York, 1997, pp. 307–326.
34 G. M. Sheldrick, in SHELXS97, Program for Crystal Structure Determination, University of Gottingen, 1997.
35 J. A. S. Howell and P. M. Burkinshaw, *Chem. Rev.*, 1983, **83**, 557.
36 S. K. Malik and A. Poë, *Inorg. Chem.*, 1979, **18**, 1241.
37 L. Chen and A. J. Poë, *Can. J. Chem.*, 1989, **67**, 1924.
38 R. H. E. Hudson and A. J. Poë, *Inorg. Chim. Acta*, 1997, **259**, 257.
39 A similar argument could be applied to the bridge closing reaction of $[Rh_6(CO)_{15}(\kappa^1\text{-P(pyrrolyl)}_3)]$ which has otherwise been concluded to involve simple CO dissociation.[40] Some C–Rh bond-making may well be occurring.
40 C. Babij, C. S. Browning, D. Farrar, H., I. O. Koshevoy, I. S. Podkorytov, A. J. Poë and S. P. Tunik, *J, Am. Chem. Soc.*, 2002, **124**, 8922.
41 A. Poë and V. C. Sekhar, *J. Am. Chem. Soc.*, 1984, **106**, 5034.
42 M. C. Barral, R. Jimenez-Aparicio, R. Kramolowsky and I. Wagner, *Polyhedron*, 1993, **12**, 903.
43 S. P. Tunik, A. V. Vlasov, N. I. Gorshkov, G. L. Starova, A. B. Nikol'skii, M. I. Rybinskaya, A. S. Batsanov and Y. T. Struchkov, *J. Organomet. Chem.*, 1992, **433**, 189.
44 N. K. Kiriakidou-Kazemifar, M. J. Stchedroff, M. A. Mottalib, M. H. Johansson, M. Monari, S. Selva, and E. Nordlander, unpublished results.
45 M. G. Choi, L. M. Daniels and R. J. Angelici, *Inorg. Chem.*, 1991, **30**, 3647.
46 R. A. Sanchez-Delgado, V. Herrera, C. Bianchini, D. Masi and C. Mealli, *Inorg. Chem.*, 1993, **32**, 3766.
47 D. G. Dick and D. W. Stephan, *Can. J. Chem.*, 1986, **64**, 1870.
48 S. P. Tunik, A. V. Vlasov, K. V. Kogdov, G. L. Starova, A. B. Nikolskii, O. S. Manole and Y. T. Struchkov, *J. Organomet. Chem.*, 1994, **479**, 59.
49 S. L. Schiavo, F. Faraone, M. Lanfranchi and A. Tiripicchio, *J. Organomet. Chem.*, 1990, **387**, 357.
50 G. Bruno, S. Lo Schiavo, E. Rotondo, C. G. Arena and F. Faraone, *Organometallics*, 1989, **8**, 886.
51 R. E. Marsh, *Acta Crystallogr., Sect. B*, 1997, **53**, 317.
52 G. A. Acum, M. J. Mays, P. R. Raithby and G. A. Solan, *J. Organomet. Chem.*, 1996, **508**, 137.
53 R. Gobetto, E. Sappa, A. Tiripicchio, M. T. Camellini and M. J. Mays, *J. Chem. Soc., Dalton Trans.*, 1990, 807.
54 A. Z. Voskoboynikov, M. A. Osina, A. K. Shestakova, M. A. Kazankova, I. G. Trostyanskaya, I. P. Beletskaya, F. M. Dolgushin, A. I. Yanovsky and Y. T. Struchkov, *J. Organomet. Chem.*, 1997, **545–546**, 71.
55 S. P. Tunik, I. S. Podkorytov, B. T. Heaton, J. A. Iggo and J. Sampanthar, *J. Organomet. Chem.*, 1998, **550**, 221.
56 M. Sawamura, H. Hamashima, M. Sugawara, R. Kuwano and Y. Ito, *Organometallics*, 1995, **14**, 4549.
57 E. Lindner, H. Rauleder, C. Scheytt, H. A. Mayer, W. Hiller, R. Fawzi and P. Wegner, *Z. Naturforsch., Teil B*, 1984, **39**, 632.
58 C. Santelli-Rouvier, C. Coin, L. Toupet and M. Santelli, *J. Organomet. Chem.*, 1995, **495**, 91.
59 *Pure Appl. Chem.*, 1976, **45**, 11.
60 R. S. Cahn, C. K. Ingold and V. Prelog, *Angew. Chem., Int. Ed. Engl.*, 1966, **5**, 385.
61 V. Prelog and G. Helmchen, *Angew. Chem., Int. Ed. Engl.*, 1982, **21**, 567.
62 K. Mikami, M. Terada, T. Korenaga, Y. Matsumoto and S. Matsukawa, *Acc. Chem. Res.*, 2000, **33**, 391.
63 K. Mikami, T. Korenaga, T. Ohkuma and R. Noyori, *Angew. Chem., Int. Ed.*, 2000, **39**, 3707.
64 K. Mikami, M. Terada, T. Korenaga, Y. Matsumoto, M. Ueki and R. Angelaud, *Angew. Chem., Int. Ed.*, 2000, **39**, 3532.